Mutations Pro → Ala-35 and Tyr → Phe-75 of *Rhodobacter capsulatus* Ferrocytochrome c_2 Affect Protein Backbone Dynamics: Measurements of Individual Amide Proton Exchange Rate Constants by ^1H–^{15}N HMQC Spectroscopy†

Paul R. Gooley,‡,§ Michael S. Caffrey,‖ Michael A. Cusanovich,‖ and Neil E. MacKenzie*,‡

Department of Pharmaceutical Sciences, College of Pharmacy, and Department of Biochemistry, University of Arizona, Tucson, Arizona 85721

Received July 15, 1991; Revised Manuscript Received September 26, 1991

ABSTRACT: Comparisons of hydrogen–deuterium solvent exchange rate constants for the NH protons of wild-type Pro → Ala-35 (P35A) and Tyr → Phe-75 (Y75F) *Rhodobacter capsulatus* ferrocytochromes c_2 were made by ^1H–^{15}N heteronuclear multiple-quantum correlation spectroscopy. Exchange rate constants increased for the NH protons of residues 45–46, 54, 57–58, 60–61, 82–87, 98, and 100 with Y75F and 16–18, 20, 34, 37, 43, 45–46, and 58 with P35A. The increases in exchange rate constants are consistent with changes in unfolding equilibria and protein dynamics. In Y75F the exchange rate constants of the observable NH protons of the helix spanning Pro-79–Asp-89, namely Phe-82–Leu-87, increase to a similar degree, suggesting that this helix is a single cooperative unfolding unit compatible with the local unfolding model. As the oxidation–reduction potential of Y75F is 59 mV lower than wild-type cytochrome c_2 (367 mV), the dynamic changes in this mutant, compared to wild-type, are proposed to be important determinants of the oxidation–reduction potential. Several differences between wild-type and Y75F are in common with P35A, a mutation which does not affect the oxidation–reduction potential, implying that not all observed dynamic changes are functionally important.

Site-directed mutagenesis offers a means of investigating the complex problem of the contribution of individual amino acids to protein stability (Alber, 1989). Although proteins are functionally and structurally tolerant to most mutations, many mutations result in a subtle repacking of residues that is not localized to the immediate microenvironment of the mutation but whose effects are propagated throughout the protein (Loll & Lattman, 1990; Alber et al., 1988). This latter observation stresses the complexity of the contribution of an individual residue to the stabilization of a protein as small reorientations will tend to alter the forces, for example, hydrophobic, electrostatic, and hydrogen bonding, that stabilize the protein. Therefore, a complete understanding of the influence of an individual amino acid residue over the stability of a protein will require an array of techniques that can probe these forces.

The analysis of individual hydrogen–deuterium exchange rate constants of NH protons provides detailed information about the stability of hydrogen-bonded secondary and tertiary structure. These analyses have proved useful in testing the dependence of the stability of a protein on environmental conditions, such as pH, temperature, and ligand binding (Wagner, 1983; Dempsey, 1986a; Linse et al., 1990). Measurement of amide exchange rate constants of stability mutants offers a means to probe changes in local protein stabilization. The mechanism of solvent exchange of an NH proton can be expressed in the following reaction (Hvidt & Nielsen, 1966):

$$\mathrm{N(H)} \underset{k_f}{\overset{k_u}{\rightleftharpoons}} \mathrm{O(H)} \xrightarrow[\mathrm{D_2O}]{k_c} \mathrm{O(D)} \underset{k_u}{\overset{k_f}{\rightleftharpoons}} \mathrm{N(D)} \qquad (1)$$

where N is the native or closed state, O includes all the unfolded or open states of the protein and k_c, k_u, and k_f are the intrinsic (Molday et al., 1972), unfolding, and folding rate constants respectively. When $k_f \gg k_u$ the experimentally measured NH exchange rate constant (k_m) is given by (Hvidt & Nielsen, 1966)

$$k_m = (k_u k_c)/(k_f + k_c) \qquad (2)$$

Under experimental conditions where the protein is in its native conformation, $k_f \gg k_c$ (EX_2 limit) and NH proton exchange is uncorrelated (Hvidt & Nielsen, 1966; Roder et al., 1985); thus

$$k_m = (k_u/k_f)k_c = K_{op}k_c \qquad (3)$$

where K_{op} is the local unfolding equilibrium constant. Under these conditions of protein stability, localized unfolding events appear to be important for solvent exposure and exchange (Englander & Kallenbach, 1984). For example, in helices the exchange of a hydrogen-bonded NH proton that stabilizes the helix requires the breaking of the preceding hydrogen bond or bonds, and thus segments of helices or entire helices act as cooperative unfolding units. Generally, similar exchange rate constants for NH protons that are within a piece of secondary structure, but distributed both on the surface and in the interior of the protein, have been suggested to belong to local unfolding units (Wagner & Wüthrich, 1982; Englander et al., 1983; Kuwajima & Baldwin, 1983; Wüthrich et al., 1984; Wand et al., 1986). This poor correlation between exchange rate constant of the NH proton and its relative position to the protein surface is not easily reconciled with solvent penetration models (Englander & Kallenbach, 1984). More convincing

† This work was supported by the Arizona Research Laboratories Division of Biotechnology and by Grants BRSGS07-RR07002, RR05605, and GM21277 from the National Institutes of Health.

* Address correspondence to this author.

‡ Department of Pharmaceutical Sciences.

§ Present address: Merck Sharpe & Dohme Research Laboratories, Rahway, NJ 07065.

‖ Department of Biochemistry.

0006-2960/92/0431-443$03.00/0

evidence of local unfolding phenomena was obtained by comparing the exchange rates of seven sequential NH protons, distributed on the solvent-exposed and protein-buried faces of the F–FG helix, in carboxyhemoglobin to deoxyhemoglobin (Englander et al., 1983). The change in state between deoxyhemoglobin and carboxyhemoglobin increases the exchange of all seven NH protons 30-fold.

The free energy difference ΔG_{op} between the open and closed forms can be calculated from K_{op} (Wand et al., 1986):

$$\Delta G_{op} = -RT \ln K_{op} \quad (4)$$

When differences in ΔG_{op} for the respective exchange rate constants of an NH proton in two forms of a protein are compared, for example, a wild-type and mutant protein, changes to the equilibrium of localized unfolding can be measured:

$$\delta\Delta G_{op} = -RT\delta(\ln K_{op}) = -RT \ln (k_m^1/k_m^2) \quad (5)$$

where k_m^1 and k_m^2 are the exchange rate constants for the same NH proton in the two forms of a protein. In this idealized situation an assumption has been made; that is, for exchange to occur in the open states by k_c, near complete unfolding is required. Even if this is not true, provided that the exchange of respective protons occurs in the same unfolded conformation for the two forms of the protein, $\delta\Delta G_{op}$ will reflect differences in only the unfolding equilibria. However, if these open states differ, exchange will occur by different apparent intrinsic rate constants, k_c^{app1} and k_c^{app2}, where $k_c^{app1} \neq k_c^{app2} < k_c$, for example, when the open states of the mutant and wild-type differ structurally or when the solvent accessible surface of the open state differs. Thus, interpretations of $\delta\Delta G_{op}$ must be approached with caution, but their significance may be that they point to functionally important regions of the protein (Englander et al., 1983; Wand et al., 1986).

We have been engaged in an intensive study of wild-type and various mutants of *Rhodobacter capsulatus* cytochrome c_2, a member of the class I *c*-type cytochromes, to test hypotheses concerning the role of individual residues in phenomena such as structure, oxidation–reduction potential, and kinetics of electron transfer (Cusanovich et al., 1988). Although there is minimal amino acid sequence homology among the cytochromes *c*, significant structural homology is observed between the individual members. Importantly, the protein fold results in a hydrophobic environment around the heme to give these cytochromes a high oxidation–reduction potential, thus favoring electron retention (Kassner, 1972). Despite this structural homology, the oxidation–reduction potentials of the cytochromes *c* range from about 20 to 500 mV (Cusanovich et al., 1988), indicating that other subtle interactions have an important function in controlling oxidation–reduction potential.

The NMR[1] spectra of the wild-type and two mutants of *R. capsulatus* cytochrome c_2, Pro → Ala-35 (P35A) and Tyr → Phe-75 (Y75F), have been extensively analyzed (Gooley et al., 1990, 1991a,b, and unpublished results). Analysis of NOE data indicates that the secondary and tertiary structures of the wild-type cytochrome c_2 are similar to those of other members of the class I *c*-type cytochromes. The significance of the strictly conserved Pro-35 is suggested to be the constraint of the protein backbone for the carbonyl of Pro-35 to form a hydrogen bond with the $N_\pi H$ of His-17 (Takano & Dickerson, 1981a). However, analysis of NMR spectra of P35A indicates that the mutation does not appear to perturb the structure of the protein and that the hydrogen bond between the carbonyl of Ala-35 and the $N_\pi H$ of His-17 is intact (Gooley & MacKenzie, 1990; Gooley et al., 1991a). The OH group of Tyr-75 is probably hydrogen bonded to a bound water molecule (Caffrey et al., 1991), and, although this hydrogen bond is undoubtedly disrupted in Y75F, analysis of the NMR spectra of this protein has yet to reveal a significant structural perturbation (Gooley et al., unpublished results). This latter mutation decreases the oxidation–reduction potential by 59 mV compared to wild-type (368 mV), and solvent denaturation studies show that reduced Y75F is 1.8 kcal·mol^{-1} less stable than reduced wild-type while oxidized Y75F is as stable as oxidized wild-type (Caffrey et al., 1991). These data are comparable to a recent report of a similar mutant of rat cytochrome *c*; however, in this latter case preliminary NOE data infer that there is a reorganization of side chains (Luntz et al., 1989). In contrast to Y75F, the oxidation–reduction potential of P35A is similar to that of wild-type, and both reduced and oxidized P35A are 2 kcal·mol^{-1} less stable than the reduced and oxidized wild-type (Caffrey, 1991).

We are reporting here the hydrogen–deuterium exchange rate constants for the reduced forms of wild-type, Y75F, and P35A *R. capsulatus* cytochromes c_2. Analysis of differences show localized effects in both mutant proteins, and, in the case of Y75F, the perturbed regions are in common with a recent study (Gooley et al., 1991b) where the exchange rate constants of the oxidized and reduced *R. capsulatus* cytochrome c_2 were compared. From these data, we conclude that the dynamics of these regions are important in the maintenance of the oxidation-reduction potential of the cytochrome c_2. In addition, cooperative localized unfolding is demonstrated for the α-helical region Phe-82 to Leu-87 in Y75F.

Materials and Methods

Protein Purification and Sample Preparation. The preparation and purification of ^{15}N-enriched cytochrome c_2 with $(^{15}NH_4)_2SO_4$ (Isotech, Inc.) has been described previously (Gooley et al., 1990). Samples of 2 mM wild-type, Y75F, or P35A cytochrome c_2 in 50 mM phosphate, pH 6, were reduced by sodium dithionite. The reductant was subsequently removed by repeated ultrafiltration at 4 °C. In preparation for the exchange study, samples were exchanged three times by ultrafiltration with 0.5–1-mL aliquots of 50 mM phosphate and 2 mM dithiothreitol in D_2O at pH 6 (pH meter reading) and 4 °C. Before the NMR tube was capped, the samples were flushed with argon.

NMR Spectroscopy. The experimental procedure for acquiring and processing ^1H–^{15}N HMQC to obtain hydrogen–deuterium NH exchange rate constants was similar to a previous report (Gooley et al., 1990). Samples were exchanged with the above D_2O buffer for 40 min at 4 °C and then placed in the spectrometer. After 10 min of temperature equilibration at 30 °C, the first spectrum was acquired. ^1H–^{15}N HMQC spectra (Bax et al., 1983) were acquired with spectral widths of 5000 (^1H) and 2000 Hz (^{15}N) and 100 t_1 points. Acquisition times of 24 min (8 scans; 2 dummy scans) were used for spectra up to 1000 min of exchange and 38 min (16 scans; 2 dummy scans) between 1000 and 80 000 min of exchange. The time period between acquisitions was gradually increased, but not exponentially, as the exchange rate constants vary by at least seven orders of magnitude. Samples were reequilibrated with fresh buffer every 8 days; and as the cytochrome c_2 is colored, the reequilibration process caused minimal sample losses.

Spectra were processed on a VAX 8600 using FTNMR (Hare

[1] Abbreviations: NMR, nuclear magnetic resonance; P35A, Pro → Ala-35 *R. capsulatus* cytochrome c_2; Y75F, Tyr → Phe-75 *R. capsulatus* cytochrome c_2; HMQC, heteronuclear multiple-quantum correlation.

Research). Prior to 2D Fourier transformation, the data were multiplied by shifted sine bells in both t_1 and t_2 and zero filled to yield a matrix 1024 × 1024 of real data points. Peak volumes were calculated manually by two methods. The first method used the subcommand "t", assuming an elliptical peak shape. The second method used the subcommand "i" and thus a square foot print, where the radius was equal to half the peak width at the base of the peak in the ^{1}H dimension. The first method proved unsatisfactory where peaks overlap or are not well resolved, whereas the second method did not calculate the total peak volume. Rate constants derived from either method were not significantly different; and as the second method allowed calculation of rate constants for almost all of the peaks, these values are used in this paper. In one-dimensional amide exchange studies, the intensity of the resolved N(1)H of Trp-67 does not change after 80000 min of exchange; therefore, this resonance was used as an internal standard. During these studies, the exchange rate constant of the resolved $N_\pi H$ of His-17 was calculated (Gooley & MacKenzie, 1990). Measurement of the exchange rate constant of this proton in the two-dimensional studies served as an additional check on the methods of calculation. Rate constants were calculated by exponential least-squares analysis of plots of $I = A_0 e^{-k_m t}$, where I is the measured peak volume, A_0 is the initial peak volume, k_m is the exchange rate constant (min^{-1}), and t is time (min). All measured peak volumes were used in the calculations.

Results and Discussion

NH Exchange of Reduced Wild-Type and Y75F Cytochromes c_2. All the NH protons of *R. capsulatus* cytochrome c_2 have been completely assigned (Gooley et al., 1990); therefore, within the time constraints of the two-dimensional HMQC experiment and our experimental protocol, the hydrogen–deuterium exchange rate constant of any NH proton that exchanges with a value smaller than approximately 0.05 min^{-1} can be measured. The exchange rate constants of all these NH protons for wild-type and Y75F *R. capsulatus* cytochromes c_2 are given in Table I. Within the limits of the resolution of these experiments, 15 NH protons exchange significantly faster ($k_m^{mutant}/k_m^{wild} > 2$) in Y75F than in wild-type. These protons are from residues 45–46, 54, 57–58, 60–61, 82–87, 98, and 100. To facilitate interpretation, the sequence positions where there were significant changes are shown in boldface in Table I. In addition, the NH proton of Ile-19 appears to exchange significantly slower ($k_m^{mutant}/k_m^{wild} < 2$) in Y75F than in wild-type. It is uncertain whether this latter observation is significant, particularly as the NH proton of Ile-19 is not spatially near other NH protons whose exchange rates have been affected (Figure 1).

Residues 82–87 belong to helix III, which spans Pro-79–Asp-88, inclusive (Gooley et al., 1990; Figure 1). Representative plots of the NH exchange rates of these protons are shown in Figure 2. As the first three residues of an α-helix do not form hydrogen bonds that stabilize the helix, the NH protons of Gly-80 and Ala-81 are not considered a part of helix III, implying that their exchange rate constants are not dependent on the stability of this helix. The similar increase in exchange rate constants and thus $\delta\Delta G_{op}$ (Table I) for the NH protons of residues 82–87 is convincing evidence that the entire helix is a single cooperative unfolding unit and that the mutation directly affects the unfolding equilibrium of this helix. This perturbation of an unfolding equilibrium is similar to the shift in the unfolding equilibrium for the F–FG helix in deoxyhemoglobin compared to carboxyhemoglobin (Englander et al., 1983). Notably, residues 82–87 in cytochrome c_2 span

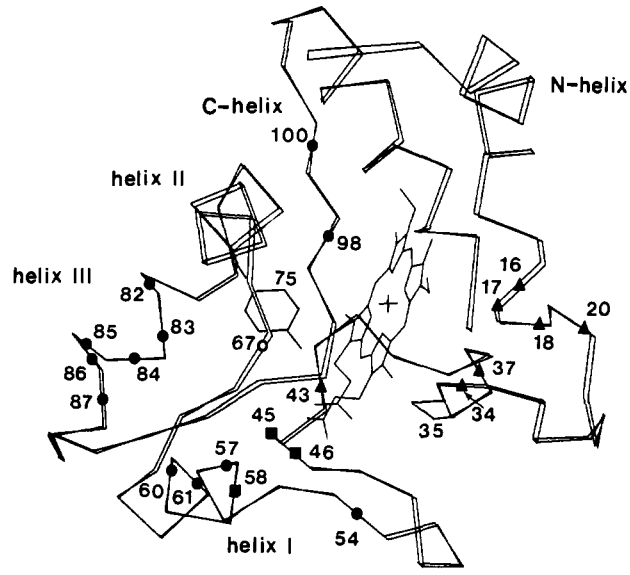

FIGURE 1: Ribbon model of *R. capsulatus* cytochrome c_2 based on the X-ray crystal coordinates of *R. rubrum* cytochrome c_2 (Bhatia, 1981). The heme and the side chains of Pro-35 and Tyr-75 are shown. The probable location of Trp-67, whose ring shows a large number of long-range NOEs (Gooley et al., 1991b), is indicated. NH protons that show different exchange rate constants ($k_m^{mutant}/k_m^{wild\text{-}type} > 2$) in wild-type compared to Y75F (●), P35A (▲), and both Y75F and P35A (■) are indicated.

almost two turns of helix III and are distributed on both the surface and in the interior of the protein (Figure 1). This distribution, however, does not influence $\delta\Delta G_{op}$, supporting the hypothesis that the exchange rate of an NH proton does not correlate with its position relative to the protein surface (Englander & Kallenbach, 1984). Structurally, the OH of Tyr-75 does not appear to be directly involved with helix III nor does the mutation to Phe appear to affect the structure of the individual hydrogen bonds of this helix. Indeed, a comparison of the chemical shifts of the proton resonances of this helix for Y75F and wild-type shows that the NH protons differ by 0.01–0.09 ppm and that the αH protons differ by 0.01–0.04 ppm (Gooley et al., unpublished), suggesting that the length of the hydrogen bonds of this helix have not been significantly altered and certainly none have been broken (Pardi et al., 1983). Therefore, other interactions, possibly between side chains of helix III and other side chains, have been disrupted, leading to the difference in local stability of helix III.

Ile-57, Val-58, Leu-60, and Gly-61 belong to the short α-helix spanning Asp-55–Gly-64, inclusive (Gooley et al., 1990; Figure 1). As Ile-57 is the third residue of this α-helix, it is not expected to be important for the stability of this helix. Evidently, the exchange rate constants of the NH protons of Ala-59 and -62 are not affected (Table I), implying either that this helix is not a single cooperative unfolding unit or that the changes in exchange rate constants for the NH protons of Val-58, Leu-60, and Gly-61 are due to structural or solvent accessibility differences. Examination of the exchange rate constants of the helices of cytochrome c_2 may serve as a guide in resolving this problem. The exchange rate constants can be divided into two categories: first, where the individual exchange rate constants decrease to a minimum as one moves from the N or C terminus of the helix toward its center, for example, helix III and the C-terminal helix, and second, where as one moves along the helix, there are a number of minima with increases and decreases in the exchange rate constants, for example, helix I and II. As the data infer that helix III

Table I: Hydrogen–Deuterium Exchange Rate Constants (k_m) and Free Energy Differences of Exchange ($\delta\Delta G_{op}$) for the NH Protons of Wild-Type, Pro → Ala-35 (P35A), and Tyr → Phe-75 (Y75F) *R. capsulatus* Ferrocytochrome c_2 at pH 6 and 30 °C[a]

		Y75F		P35A		
residue	wild-type k_m (10^{-3} min^{-1})	k_m (10^{-3} min^{-1})	$\delta\Delta G_{op}$ (kcal·mol^{-1})	k_m (10^{-3} min^{-1})	$\delta\Delta G_{op}$ (kcal·mol^{-1})	2° structure[b]
E7	18	20	0.1	16	−0.1	N-terminal helix
K8	>50	>50		>50		
F10	6.3	3.8	−0.3	≈10[c]	≈0.3	
C13	5.6	4.7	−0.1	5.1	−0.1	
K14	2.4	1.0	−0.5	2.2	−0.1	
C16	10.6[d]	20[d]	0.4	**>50**	**>0.6**	
H17	<0.001	<0.001		**0.0029**[e]	**>0.6**	
$H17^{N_\pi H}$	0.0062	0.0038	−0.3	**0.22**	**2.1**	
S18	0.24	0.28	0.1	**0.64**	**0.6**	
I19	1.8	**0.51**	**−0.8**	1.8	0.0	Ω-loop
I20	0.23	0.25	0.1	**1.3**	**1.0**	
A21	0.29	0.30	0.02	0.46	0.3	
I27	11	8.8	−0.1	12	0.1	
V28	1.7	2.2	0.2	2.5	0.2	
G34	0.62	0.52	−0.1	**≫50**	**2.6**	
L37	<0.001	<0.001		**0.0092**	**>1.3**	
Y38	0.24	0.32	0.2	0.54	0.5	type II turn
V40	7.4	6.5	−0.08	6.3	−0.1	
V41	2.7	2.3	−0.1	2.4	−0.1	
G42	1.3	0.73	−0.3	0.87	−0.2	
R43	0.0051	0.01	0.4	**0.022**	**0.9**	type II turn
A45	0.0031[e]	**0.013**	**0.9**	**0.037**	**1.5**	
G46	0.0058	**0.026**	**0.9**	**0.074**	**1.5**	
T47	0.17	0.22	0.2	0.19	0.1	
F51	>50	>50		>50		
K54	20	**>50**	**>0.6**	9	−0.5	
I57	0.40	**3.1**	**1.2**	0.36	−0.1	helix I
V58	0.0020[e]	**0.010**	**1.0**	**0.0075**	**0.8**	
A59	0.47	0.65	0.2	0.24	−0.4	
L60	<0.001	**0.0030**[e]	**0.7**	0.0010[e]		
G61	0.017	**0.044**	**0.6**	0.026	0.3	
A62	0.55	0.77	0.2	0.52	−0.03	
F65	>50	>50		>50		
W67	<0.001	<0.001		<0.001		
T68	0.24	0.30	0.1	0.24		
D71	>50	>50		>50		
I72	<0.001	<0.001		<0.001		helix II
A73	0.027	0.015	−0.4	0.025	−0.05	
T74	1.4	1.2	−0.1	1.6	0.1	
Y75	0.0026[e]	0.0019[e]	−0.2	0.0015[e]	−0.3	
V76	<0.001	<0.001		<0.001		
K77	<0.001	<0.001		<0.001		
D78	0.011	0.020	0.4	0.013	0.1	
G80	30[d]	≫50	>0.3	38[d]	0.1	helix III
A81	21	27	0.2	21	0.0	
F82	0.018	**0.12**	**1.1**	0.020	0.1	
L83	0.035	**0.39**	**1.5**	0.044	0.1	
K84	0.0096	**0.13**	**1.6**	0.0097	0.01	
E85	0.47	**3.7**	**1.2**	0.57	0.1	
K86	0.84	**5.5**	**1.1**	0.87	0.02	
L87	1.5	**23**	**1.6**	2.0	0.2	
D89	>50	>50		>50		
F98	11	**>50**	**>0.9**	12	0.1	
L100	0.070	**0.22**	**0.7**	0.086	0.1	
V107	>50	>50		>50		C-terminal helix
A108	0.35	0.39	0.1	0.46	0.2	
A109	0.045	0.039	−0.1	0.048	0.04	
Y110	0.0022[e]	0.0039[e]	0.3	0.0019[e]	−0.1	
L111	<0.001	<0.001		<0.001		
A112	0.015	0.011	−0.2	0.013	−0.1	
S113	1.0	0.97	−0.02	1.2	0.1	
V114	36	34[c]	−0.03	39[d]	0.1	
V115	41	>50	>0.1	>50	>0.1	

[a] The estimated standard deviation for individual rate constant calculations is ±10%. However, three experiments have been conducted for wild-type where exchange rate constants for 19 peaks exchanging at rate constants between 0.1 and 3 × 10^{-3} min^{-1} are possible. Standard deviations for the calculated values of these experiments range from ±5 to ±35%. Therefore, in comparing exchange rate constants and free energy differences of the mutant proteins to wild-type, only values that give a free energy difference of more than 0.5 kcal·mol^{-1} are considered significant. For rate constants shown as >0.05 min^{-1}, a peak was observed for one or two time points. For rate constants given as ≫0.05 min^{-1}, the peak was observed in wild-type but not in one of the mutants. For rate constants <0.001 min^{-1}, no appreciable change in the intensity of the proton was observed over the course of the experiment. [b] Elements of secondary structure are based upon sequential and short-range NOE analysis (Gooley et al., 1990). The C-terminal limit of the N-terminal helix is based upon analogy with other class I *c*-type cytochromes (Bhatia, 1981; Takano & Dickerson, 1981a; Bushnell et al., 1990; Louie & Brayer, 1990). [c] Phe-10 is poorly resolved from Lys-86 in P35A. [d] Only three or four points are observed in the course of the experiment. [e] Over the course of the experiment, the intensity of these amide protons reduce by 20–25%.

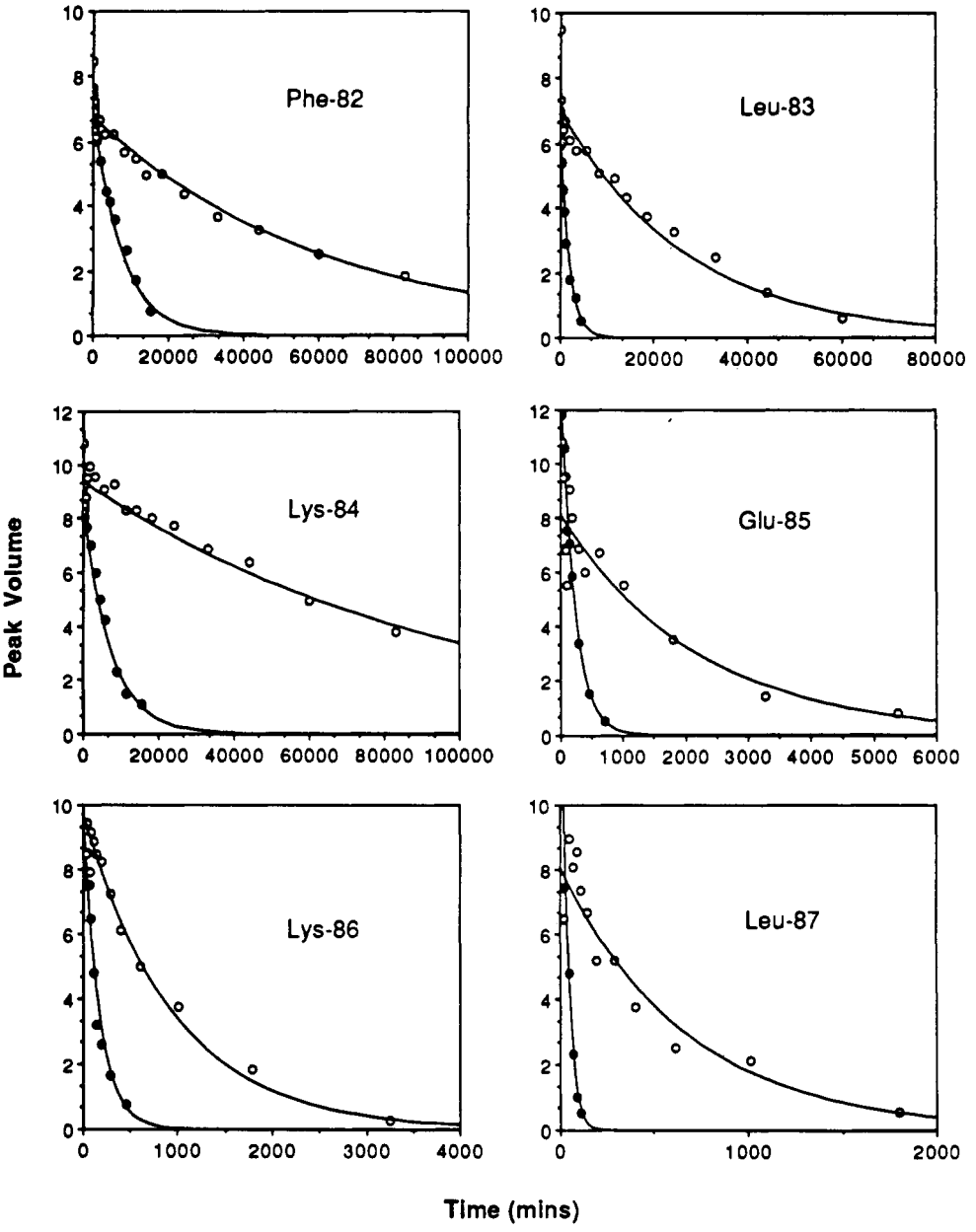

FIGURE 2: Change in peak volume versus time for the helix segment Phe-82–Leu-87 in wild-type (○) and Y75F (●) *R. capsulatus* cytochromes c_2. The data were fitted to single exponentials.

is a single cooperative folding unit and helix I is not, it is hypothesized that these minima may correlate with unfolding units.

The remaining NH protons that show increased exchange rate constants in Y75F, namely, those of residues 45–46, 54, 98, and 100, are from nonregular secondary structural regions and, therefore, must be important in stabilizing tertiary structure. As a change in the exchange rate constant of an NH proton may indicate a perturbation to either hydrogen-bond partner, it is worthwhile considering the probable oxygen acceptors of these NH protons. The extensive structural homology of the class I *c*-type cytochromes would suggest that many hydrogen bonds are conserved. Comparing the structures of *Rhodospirillium rubrum* cytochrome c_2 and tuna, horse, and yeast cytochromes *c* (Bhatia, 1981; Takano & Dickerson, 1981a; Bushnell et al., 1990; Louie & Brayer, 1990) infers that the above slowly exchanging NH protons of *R. capsulatus* cytochrome c_2 participate in the following hydrogen bonds: Ala-45(NH)–Phe-65(CO), Gly-46(NH)–heme propionate 7, Lys-54(NH)–heme propionate 6, and Leu-100-(NH)–Val-76(CO). An analogous hydrogen bond involving the NH proton of Phe-98 is not apparent. As these NH protons do not belong to defined segments of structure, it is difficult to determine whether an unfolding equilibrium or structural perturbation has occurred. However, it is noted that $\delta\Delta G_{op}$ calculated for the NH of Ala-45 and Gly-46 are the same, 0.9 kcal·mol^{-1}, inferring that these two groups may belong to the same unfolding unit.

A recent comparison of the NH exchange rate constants of reduced and oxidized *R. capsulatus* cytochrome c_2 defined a number of regions where significant differences in free energy ($\delta\Delta G_{op} > 1.5$ kcal·mol^{-1}, for reduced less oxidized) are observed, specifically for: Lys-14, His-17, Ser-18, Gly-34, Leu-37, Arg-43, Ala-45, Gly-46, Ile-57, Val-58, Leu-60, Gly-61, Val-76, Lys-77, Phe-82–Leu-87, and Leu-100 (Gooley et al., 1991b). The relative differences observed in reduced Y75F as compared to reduced wild-type closely parallel these changes for Arg-43, Ala-45, and Gly-46, those of helix II, Ile-57, Val-58, Leu-60, and Gly-61, and those of helix III, Phe-82–Leu-87 and Leu-100, indicating that the mutation has

resulted in a reduced form of the cytochrome c_2 that substantially mimics the dynamics of oxidized wild-type cytochrome c_2. These results suggest that the dynamics of these regions are important for stabilizing the reduced form of cytochrome c_2, thus contributing to the high oxidation–reduction potential (Takano & Dickerson, 1981b). Guanidine hydrochloride denaturation studies of Y75F and wild-type cytochrome c_2 are consistent with this conclusion as they demonstrate that reduced Y75F is 1.8 kcal·mol^{-1} less stable than the reduced wild-type protein, but oxidized Y75F has approximately the same stability as oxidized wild-type (Caffrey et al., 1991). Not unexpectedly, a preliminary analysis of the NH exchange rates of oxidized Y75F shows that they are similar to those of oxidized wild-type protein (Zhao et al., unpublished), supporting the conclusion that the differences in dynamics observed between the reduced forms are the most significant.

NH Exchange of Reduced Wild-Type and P35A Cytochromes c_2. In Table I, the hydrogen–deuterium exchange rate constants of all observable exchanging NH protons for wild-type and P35A *R. capsulatus* cytochromes c_2 are compared. The increased exchange rate constant for the $N_\pi H$ of His-17 in wild-type and P35A determined by one-dimensional ^1H NMR and its significance have been published elsewhere (Gooley & MacKenzie, 1990). The rate constants calculated here for this proton by two-dimensional ^1H–^{15}N methods give similar values to the previous one-dimensional experiments (0.58×10^{-5} min^{-1} for wild type; 0.22×10^{-3} min^{-1} for P35A), thus validating our technique.

In P35A 10 NH protons, assigned to residues 16–18, 20, 34, 37, 43, 45–46, and 58, exchange significantly faster than in wild-type (Table I). In contrast to Y75F, none of these protons, except Val-58, belong to residues in the helices of cytochrome c_2 (Gooley et al., 1990; Figure 1). The structural homology of the class I *c*-type cytochromes suggests that the following hydrogen bonds may be conserved: Cys-16(NH)–Cys-13(CO), His-17($N_\pi H$)–Pro-35(CO), Gly-34(NH)–Cys-16(CO), Leu-37(NH)–Ser-18(CO), Arg-43(NH)–Val-40(CO), Ala-45(NH)–Phe-65(CO), Gly-46(NH)–propionate 7, and Val-58(NH)–Lys-54(CO) (Bhatia, 1981; Takano & Dickerson, 1981a; Bushnell et al., 1990; Louie & Brayer, 1990). Analogous hydrogen bonds for the NH protons of His-17, Ser-18, and Ile-20 are not apparent. From the differences in exchange rate constants for these 10 NH protons, $\delta\Delta G_{op}$ can be calculated for 6 and estimated for 4 (Table I). As all these protons, except Val-58, are assigned to residues that are involved in nonregular secondary structure, it is difficult to determine if these residues belong to one or more folding units. In addition, the replacement of Pro-35 with Ala may have several consequences for the dynamics of the protein that require consideration. First, the rotational freedom around a peptide–Ala bond is greater than that around a peptide–Pro bond. Second, the increased ring-flip rates of Phe-51 and Tyr-53 indicate that the removal of the Pro side chain has weakened a hydrophobic core (Gooley & MacKenzie, 1990). Third, modeling the replacement of Pro-35 for Ala places a cavity in the protein surface exposing His-17, implying that there may be a change to the solvent accessible surface in the native protein near the site of mutation (Caffrey et al., unpublished results).

It is interesting to note that $\delta\Delta G_{op}$ for the $N_\pi H$ of His-17 is 2.1 kcal·mol^{-1} and that for the NH of Gly-34 is 2.6 kcal·mol^{-1}, both substantially greater than any other $\delta\Delta G_{op}$ (Table I). However, the chemical shift and NOE data are not consistent with a weakening of the hydrogen bonds of these residues, particularly the bond between the $N_\pi H$ of His-17 and the carbonyl of residue 35 which is expected to be affected by the mutation, suggesting that interactions other than these hydrogen bonds have been disrupted (Gooley & MacKenzie, 1990; Gooley et al., 1991). These latter data are in contrast to a report of structurally similar mutations in rat and *Drosophila melanogaster* cytochromes *c* where it is concluded that the hydrogen bond between the equivalent His $N_\pi H$ and Pro carbonyl is weakened (Koshy et al., 1990). The factors contributing to the $\delta\Delta G_{op}$ observed here may be, as discussed above, a combination of changes in dynamics and solvent-accessible surface. The observation of a change in ring-flip rates of Phe-51 and Tyr-53 on mutating position 35 to Ala clearly shows a weakening of a hydrophobic core that involves both these side chains and residue 35 (Gooley & MacKenzie, 1990). This change in dynamics may be the major factor in the differences in exchange rate constants and therefore $\delta\Delta G_{op}$ for P35A. For Arg-43, Ala-45, Gly-46, and Val-58, $\delta\Delta G_{op}$ ranges from 0.9 to 1.5 kcal·mol^{-1}, and as all these residues are distant from the site of mutation (>10 Å), they should not be directly influenced by the substitution of Ala for Pro. Therefore, the NH protons of these residues may report changes in unfolding equilibria. Thus, for the $N_\pi H$ of His-17 and for the NH of Gly-34, 1–1.5 kcal·mol^{-1} may be attributed to the change in the unfolding equilibrium of the hydrophobic core while the remaining 1 kcal·mol^{-1} could be due to a difference in the solvent-accessible surface of the native protein. The latter contribution suggests that, although solvent access into the native protein is not the determining factor in NH exchange, its relative importance needs to be addressed in experiments where the NH exchange rates of mutant and wild-type proteins are compared, particularly for NH protons near the protein surface and the site of mutation.

$\delta\Delta G_{op}$ for both Ala-45 and Gly-46 is 1.5 kcal·mol^{-1}, indicating that these residues may belong to the same unfolding unit. A similar observation for Y75F (Table I) supports this conclusion, although in this case $\delta\Delta G_{op}$ for Ala-45 and Gly-46 is 0.9 kcal·mol^{-1}. The difference in $\delta\Delta G_{op}$ between the two mutants for Ala-45 and Gly-46 infers that the unfolding equilibrium constant, K_{op} (eq 5), differs for this region in P35A compared to Y75F. However, it is important to note that the observed exchange rate, k_m, is a product of both k_c and K_{op} (eq 3) and thus a difference in k_c will also change k_m. In this hypothesis, the structures of the open states are ordered to a degree, that is, there are residual structures, and exchange does not occur by k_c but at a reduced rate constant k_c^{app} (Dempsey, 1986b). In the example here, the structural constraints of Pro in position 35 of cytochrome c_2, and its interactions with the side chains of Phe-51 and Tyr-53, may impose a degree of order to the open state in wild-type and Y75F that is reduced in P35A where Ala is in position 35.

The oxidation–reduction potential of P35A is 359 mV, only 8 mV less than that in wild-type, indicating that this mutation has minimal effect on the oxidation–reduction potential (Gooley et al., 1991a). Comparing $\delta\Delta G_{op}$ for reduced P35A and reduced wild-type to those of reduced and oxidized wild-type (Gooley et al., 1991b) shows, qualitatively, common differences for His-17, Ser-18, Gly-34, Leu-37, Arg-43, Ala-45, Gly-46, and Val-58. Irrespective of whether unfolding equilibria or differences in solvent accessibility are responsible for the increases in NH exchange rate constants, the differences suggest that these regions are less hydrophobic in P35A than in wild-type. Significantly, these localized changes in the hydrophobicity of the protein do not influence the oxidation–reduction potential. The remaining changes observed in

the comparison of the NH exchange rate constants of oxidized and reduced wild-type cytochrome c_2, particularly for Ile-57 and the other residues of helix II and helix III, are not observed in P35A. Comparing differences between P35A and Y75F further indicates that the dynamics of helix II and III are important factors in determining the oxidation–reduction potential and questions the relative importance of the other residues.

Comparison of $\delta\Delta G_{op}$ with $\delta\Delta G_u$, the Free Energy Difference of Unfolding. Guanidine hydrochloride denaturation experiments show that $\delta\Delta G_u$, the free energy difference of unfolding, for Y75F and P35A compared to wild-type ferrocytochrome c_2 is 1.8 and 2.0 kcal·mol^{-1}, respectively, where the mutants are less stable than wild-type (Caffrey et al., 1991; Caffrey, 1991). It is important to note that, in the solvent denaturation experiments, protein unfolding is monitored by the loss of the circular dichroism signal at 220 nm, which is characteristic for helix. In the NH exchange experiments, helices I and III are less stable in Y75F compared to wild-type, whereas all the helices are equally as stable in P35A as in wild-type ferrocytochromes c_2. The data for P35A suggest that under denaturing conditions the localized destabilization, observed in the NH exchange experiment, is propagated globally. Indeed, other NH exchange studies have demonstrated that, under denaturing conditions, the localized perturbation, observed under native conditions, is propagated throughout the protein (Wagner et al., 1984; Jandu et al., 1990). Under nondenaturing conditions, the exchange of amide protons is expected to occur by localized unfolding, and thus residual structures are expected. Therefore, $\delta\Delta G_{op}$ is not expected to be greater than the difference in the free energy of unfolding ($\delta\Delta G_u$) determined under denaturing conditions. In the NH exchange studies reported here, the largest $\delta\Delta G_{op}$ for Y75F ranges from 1.0 to 1.6 kcal·mol^{-1} for Ile-57 and Val-58 (helix I) and for Phe-82–Leu-87 (helix III). The correspondence between the guanadine hydrochloride denaturation and solvent exchange experiments on Y75F and wild-type ferrocytochromes c_2 contends that the folded and unfolded states of the region encompassing helices I and III are similar for each experiment. This latter point does not infer that the unfolded states in either experiment are fully unfolded (Pace et al., 1990). However, the largest $\delta\Delta G_{op}$ observed in the NH exchange study of P35A is greater than 2.6 kcal·mol^{-1} for Gly-34, which is significantly larger than the calculated value for $\delta\Delta G_u$ of 2.0 kcal·mol^{-1}. As discussed above, $\delta\Delta G_{op}$ can be rationalized as a combination of effects, including changes to the solvent-accessible surface of the native protein and changes in local unfolding. The importance of this observation is that it serves as a caution that a number of factors contribute to the solvent exchange of NH protons and that the interpretation of exchange rate constants for protons near the point of mutation is difficult.

Conclusion

Site-directed mutagenesis and hydrogen–deuterium exchange of NH protons offers a means of studying the effects of mutations on the dynamics of a protein. In comparison to other studies that show site-specific mutations of proteins can result in propagation of structural effects (Alber et al., 1988; Loll & Lattman, 1990), the work presented here demonstrates that mutations can also produce the propagation of dynamic effects. Such a phenomenon can be visualized in terms of the local unfolding model where a mutation can affect the unfolding equilibrium of structural entities such as an entire helix. For Y75F, the cooperative changes in exchange rate constants for the helical region spanning Phe-82–Leu-87 are an excellent example of a helix that is a single unfolding unit, compatible with the local unfolding model of NH exchange. Of the two mutants studied here, Y75F has an oxidation–reduction potential significantly lower than that of wild-type. A comparison of the differences of wild-type and Y75F to a similar investigation of reduced and oxidized wild-type *R. capsulatus* cytochrome c_2 (Gooley et al., 1991b) points to regions of the protein that may play an essential role in controlling oxidation–reduction potential: helix II, Ile-57–Phe-65 and helix III, Pro-79–Asp-89. Thus, we conclude that the propagation of dynamic effects is an important means for the control of protein stability and, in the cytochrome c_2, this influences function by controlling oxidation–reduction potential.

This study further points to the potential problems of distinguishing between changes to unfolding equilibria, relative solvent accessibility in the open state, changes to the solvent-accessible surface of the native protein, or other structural and dynamic changes. Indeed, the significant changes to the exchange rate constants of His-17 and Gly-34 in P35A remain unclear, with three possibilities contributing: (1) change in the dynamics of a hydrophobic core, (2) a structural or solvent-access difference in the unfolded states, or (3) a cavity and thus differences in solvent access of the native states. Therefore, interpretation of NH exchange data is difficult for NH protons near the site of mutation where structural differences are potentially greatest. In contrast, where exchange rates are equally affected, such as in helices, the data can be considered as having an "internal" control, and interpretation of changes to unfolding equilibria appear valid.

Acknowledgments

We thank Ms. Ellie Nielson for technical assistance and protein purification.

Registry No. Pro, 147-85-3; Ala, 56-41-7; Tyr, 60-18-4; Phe, 63-91-2; cytochrome c_2, 9035-43-2.

References

Alber, T. (1989) *Annu. Rev. Biochem. 58*, 765–798.

Alber, T., Bell, J. A., Dao-Pin, S., Nicholson, H., Wozniak, J. A., Cook, S., & Matthews, B. W. (1988) *Science 239*, 631–635.

Bax, A., Griffey, R. H., & Hawkins, B. L. (1983) *J. Magn. Reson. 55*, 301–315.

Bhatia, G. E. (1981) Ph.D. Thesis, University of California, San Diego, CA.

Bushnell, G. W., Louie, G. V., & Brayer, G. D. (1990) *J. Mol. Biol. 214*, 585–595.

Caffrey, M. S. (1991) Ph.D. Thesis, University of Arizona, Tucson, AZ.

Caffrey, M. S., Daldal, F., Holden, H., & Cusanovich, M. A. (1991) *Biochemistry 30*, 4119–4125.

Cusanovich, M. A., Meyer, T. E., & Tollin, G. (1988) in *Advances in Inorganic Biochemistry, Heme Proteins 7* (Eichhorn, G. L., & Manzilli, L. G., Eds.) pp 37–92, Elsevier, New York.

Dempsey, C. E. (1986a) *Biochemistry 25*, 3904–3911.

Dempsey, C. E. (1986b) *Eur. J. Biochem. 157*, 617–618.

Englander, S. W., & Kallenbach, N. R. (1984) *Q. Rev. Biophys. 16*, 521–655.

Englander, J. J., Rogero, J. R., & Englander, S. W. (1983) *J. Mol. Biol. 169*, 325–344.

Gooley, P. R., & MacKenzie, N. E. (1990) *FEBS Lett. 260*, 225–228.

Gooley, P. R., Caffrey, M. S., Cusanovich, M. A., & MacKenzie, N. E. (1990) *Biochemistry 29*, 2278–2290.

Gooley, P. R., Caffrey, M. S., Cusanovich, M. A., & MacKenzie, N. E. (1991a) *Eur. J. Biochem. 196*, 653–661.
Gooley, P. R., Zhao, D., & MacKenzie, N. E. (1991b) *J. Biomol. Nucl. Magn. Reson. 1*, 145–154.
Hvidt, A., & Nielsen, S. O. (1966) *Adv. Protein Chem. 21*, 287–386.
Jandu, S. K., Ray, S., Brooks, L., & Leatherbarrow, R. J. (1990) *Biochemistry 29*, 6264–6269.
Kassner, R. J. (1972) *Proc. Natl. Acad. Sci. U.S.A. 69*, 2263–2267.
Koshy, T. I., Luntz, T. L., Schejter, A., & Margoliash, E. (1990) *Proc. Natl. Acad. Sci. U.S.A. 87*, 8697–8701.
Kuwajima, K., & Baldwin, R. L. (1983) *J. Mol. Biol. 169*, 299–323.
Linse, S., Teleman, O., & Drankenberg, T. (1990) *Biochemistry 29*, 5925–5934.
Loll, P. J., & Lattman, E. E. (1990) *Biochemistry 29*, 6866–6873.
Louie, G. V., & Brayer, G. D. (1990) *J. Mol. Biol. 214*, 527–555.
Luntz, T. L., Schejter, A., Garber, E. A. E., & Margoliash, E. (1989) *Proc. Natl. Acad. Sci. U.S.A. 86*, 3524–3528.
Molday, R. S., Englander, S. W., & Kallen, R. G. (1972) *Biochemistry 11*, 150–158.
Pace, C. N., Laurents, D. V., & Thomson, J. A. (1990) *Biochemistry 29*, 2564–2572.
Pardi, A., Wagner, G., & Wüthrich, K. (1983) *Eur. J. Biochem. 137*, 445–454.
Roder, H., Wagner, G., & Wüthrich, K. (1985) *Biochemistry 24*, 7396–7407.
Takano, T., & Dickerson, R. E. (1981a) *J. Mol. Biol. 153*, 79–94.
Takano, T., & Dickerson, R. E. (1981b) *J. Mol. Biol. 153*, 95–115.
Wagner, G. (1983) *Q. Rev. Biophys. 16*, 1–57.
Wagner, G., & Wüthrich, K. (1982) *J. Mol. Biol. 160*, 343–361.
Wagner, G., Stassinopoulou, G., & Wüthrich, K. (1984) *Eur. J. Biochem. 145*, 431–436.
Wand, A. J., Roder, H., & Englander, S. W. (1986) *Biochemistry 25*, 1107–1114.
Wüthrich, K., Strop, P., Ebina, S., & Williamson, M. P. (1984) *Biochem. Biophys. Res. Commun. 122*, 1174–1178.

Experimental and Computational Infrared CD Studies of Prototypical Peptide Conformations†

Sheryl S. Birke, Ismailu Agbaje, and Max Diem*

Departments of Chemistry and Biochemistry, Hunter College, The City University of New York, 695 Park Avenue, New York, New York 10021

Received May 15, 1991; Revised Manuscript Received October 8, 1991

ABSTRACT: The infrared vibrational circular dichroism (VCD) spectral features of prototypical peptide secondary structures were reported previously by Yasui and Keiderling [Yasui, S. C., & Keiderling, T. A. (1986) *Biopolymers 25*, 5]. These results demonstrated that the "random coil" peptide conformation exhibits VCD signals which are approximately mirror-image features of those exhibited by α-helical conformers. We report here a comparison of observed VCD spectra with those computed for several secondary structures, using the extended coupled oscillator formalism employed previously to compute VCD spectra of model DNA [Zhong et al. (1990) *Biochemistry 29*, 7485]. These studies suggest that the so-called random-coil peptide conformation has distinct short-range order and appears to be a left-handed, helical structure.

The peptide backbone exists in a number of distinct and well-known conformations, determined by the value of the ϕ and ψ angles (Schulz & Schirmer, 1979). Among the most common of these conformations is the right-handed α-helix, which shows distinct CD features described by Holzwarth and Doty (1965) and Greenfield and Fasman (1969). The aforementioned angles ϕ and ψ associated with the right-handed α-helix fall into a broad minimum energy region in the Ramachandran plot for peptides, centered about −55°, −55°.

Many α-helical model peptides can be induced to undergo a phase transition by varying the acidity or the ionic strength of the solvent. Poly(L-lysine), for example, exists in an α-helical form at a pH above 10.6. When the medium is acidified, a distinct phase transition to another conformer occurs, which exhibits CD spectra which are smaller in amplitude than those of the α-helix, and are inverted in sign. This conformation has been referred to as the "random coil" form.

The first conformation-dependent VCD spectra of polyamino acids were reported by Yasui and Keiderling (1986a,b) for poly(L-tyrosine) (PLT) in DMSO, and nearly simultaneously by Keiderling's and Nafie's groups for poly(L-lysine) (PLL) in aqueous solution (Yasui & Keiderling, 1986a,b; Paterlini et al., 1986). This last study showed unequivocally that a true random conformation, obtained by denaturation of PLL, shows minimal VCD signals in the amide I′ region. On the basis of the sign pattern of the observed VCD couplet, this publication also suggested that the "random coil" conformation is actually a left-handed helical structure. VCD,

† This research was supported by the National Institute of General Medical Sciences (GM 28619). The construction of the VCD instruments was supported by grants from the NSF (CHE 86-07934), by several CUNY faculty research awards, and by Instruments, SA, Metuchen, NJ. The molecular graphics workstation was purchased through an RCMI grant (RR 03037) to the Division of Science and Mathematics at Hunter College.

* Address correspondence to this author at the Department of Chemistry, Hunter College of The City University of New York.

0006-2960/92/0431-450$03.00/0